Supporting information

Charge Generation and Mobility-Limited Performance of Bulk Heterojunction Solar Cells with a Higher Adduct Fullerene

Steffen Roland[+], Liang Yan[#], Qianqian Zhang[#], Xuechen Jiao[°], Adrian Hunt[°], Masoud Ghasemi[°] Harald Ade[°],Wei You[#§], Dieter Neher[+]

[+] Institute of Physics and Astronomy, University of Potsdam, Karl-Liebknecht-Str.24-25, D-14476 Potsdam-Golm, Germany

[#] Department of Chemistry, University of North Carolina at Chapel Hill, Chapel Hill, North Carolina 27599-3290, United States

[§] Department of Applied Physical Sciences, CB #3216, University of North Carolina, Chapel Hill, North Carolina 27599-3216, United States

[°]Department of Physics and Organic and Electronic Laboratory (ORaCEL), North Carolina State University, North Carolina 27695-7518

1. EL and EQE fitting. Determination of the radiative limit

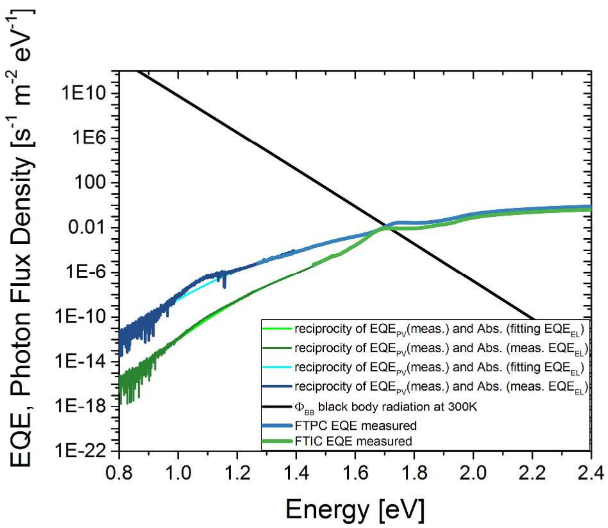

Figure S 1 External quantum efficiency (PV) measured and extrapolated to lower energy. Extrapolation either by adding the gaussian fitted EQE_{PV} to the real EQE_{PV} or by adding the calculated absorption from the measured emission spectrum.

At open circuit voltage conditions the total current is zero and the following expression for open circuit voltage can be derived. With J_0 , the dark saturation current and J_{Ph} the photocurrent (in this case approximated with the short circuit current as the generation of free charges is field independent).

$$V_{OC} = \frac{k_B T}{q} \ln\left(\frac{J_{Ph}}{J_0} + 1\right) \tag{S 1}$$

The dark saturation current is related to the emission and absorption spectra via:

$$J_0 = \frac{q}{EQE_{EL}} \int EQE_{PV}(E) \Phi_{BB}(300\ K) dE \tag{S 2}$$

In the radiative limit EQE_{EL} would be equal to unity. Therefore the radiative limit of the V_{OC} can be calculated from the EQE_{PV} and the short circuit current of each cell.

Table S1 Radiative limit of the open circuit voltage

	J_{Ph} [A m^{-2}]	$J_{0,RAD}$ [A m^{-2}]	$V_{OC,RAD}$ [V]	$EQE_{EL,int}$	V_{OC} (calc.) [V]	V_{OC} [V]
FT:PC	83	2.33E-18	1.137	2.77E-6	0.81	0.79
FT:PC (Gaussian fit)	83	1.10E-18	1.156	2.77E-6	0.83	0.79
FT:IC	47	7.21E-22	1.327	1.13E-6	0.98	1.00
FT:IC (Gaussian fit)	47	1.53E-21	1.308	1.13E-6	0.96	1.00

2. Delay dependence of generation efficiency of FT:IC

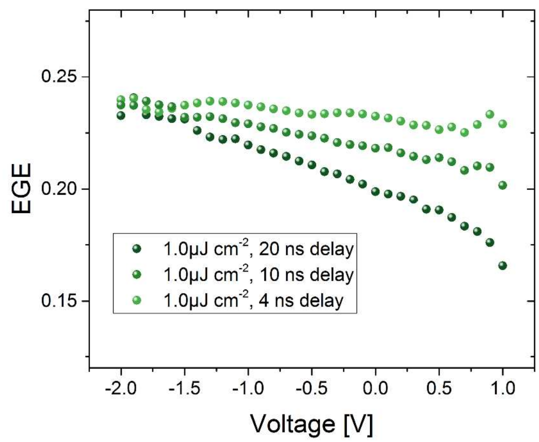

Figure S2 External generation efficiency determined from the extracted charges after different delay times.

The Apparent field dependence of generation of free charge carriers vanishes for shorter delay times. This indicates that the actual generation of free charges is not field dependent but that fast non-geminate recombination lowers the extractable amount of charges already after a few ns.

3. BACE mobility data

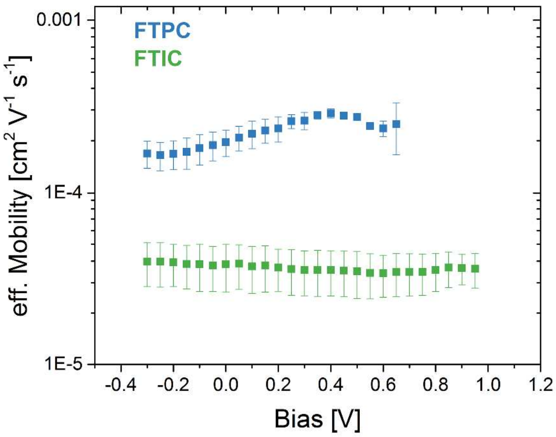

Figure S 3 Effective mobilities determined from the data depicted in Figure 3 Error! Reference source not found. **according to the work by Albrecht et al.[39] Most reliable mobility results are found close to V_{OC} conditions.**

4. SCLC mobility measurement

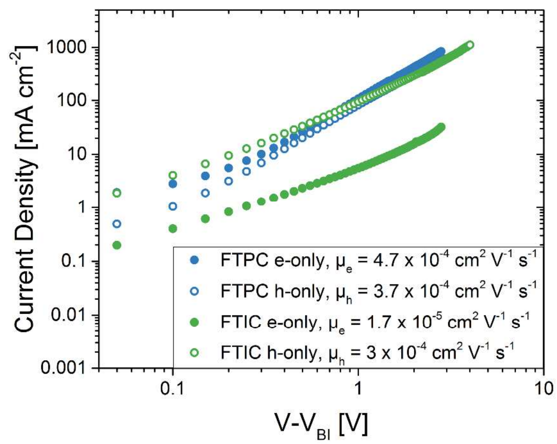

Figure S 4 Space Charge Limited Currents measured at Potsdam University for FT:PC and FT:IC electron and hole only devices.

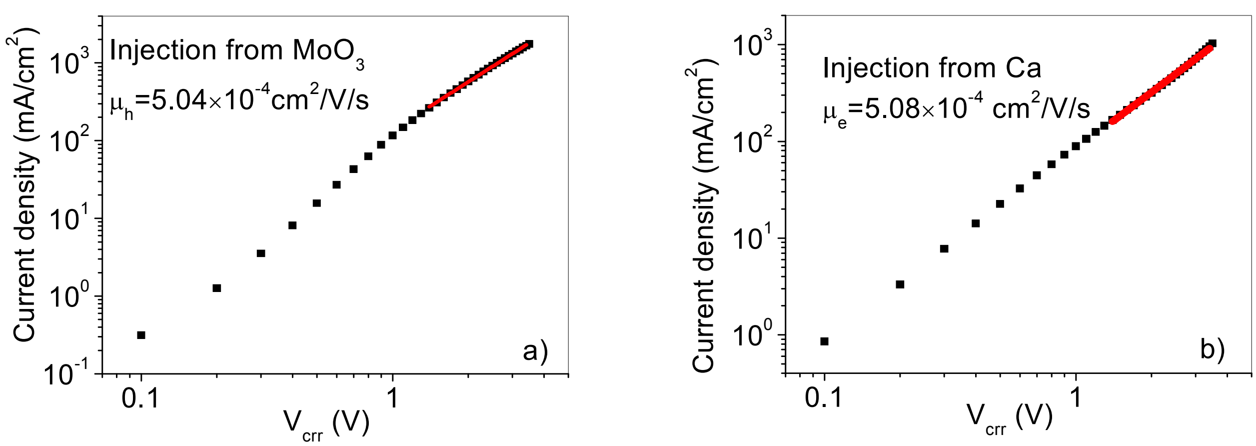

Figure S 5 Space Charge Limited Currents for a) FT:PC hole only devices and b) FT:PC electron only devices measured at UNC

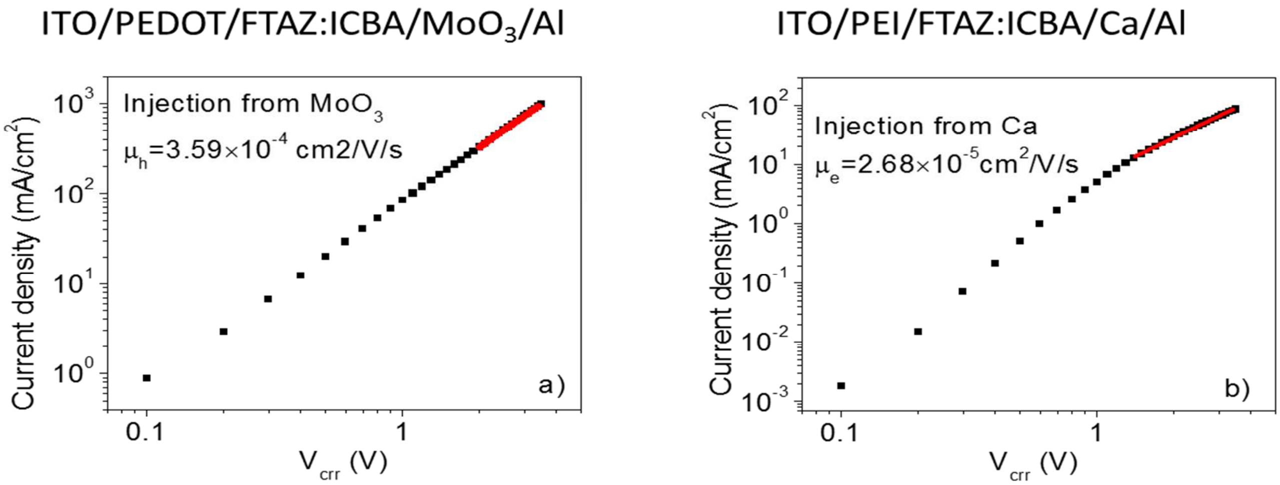

Figure S 6 Space Charge Limited Currents for a) FT:IC hole only devices and b) FT:IC electron only devices measured at UNC

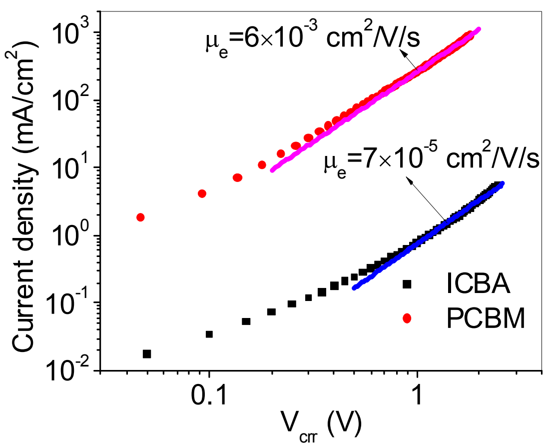

Figure S 7 Space Charge Limited Currents for ICBA and PCBM measured at UNC

5. Photoluminescence and absorption spectra

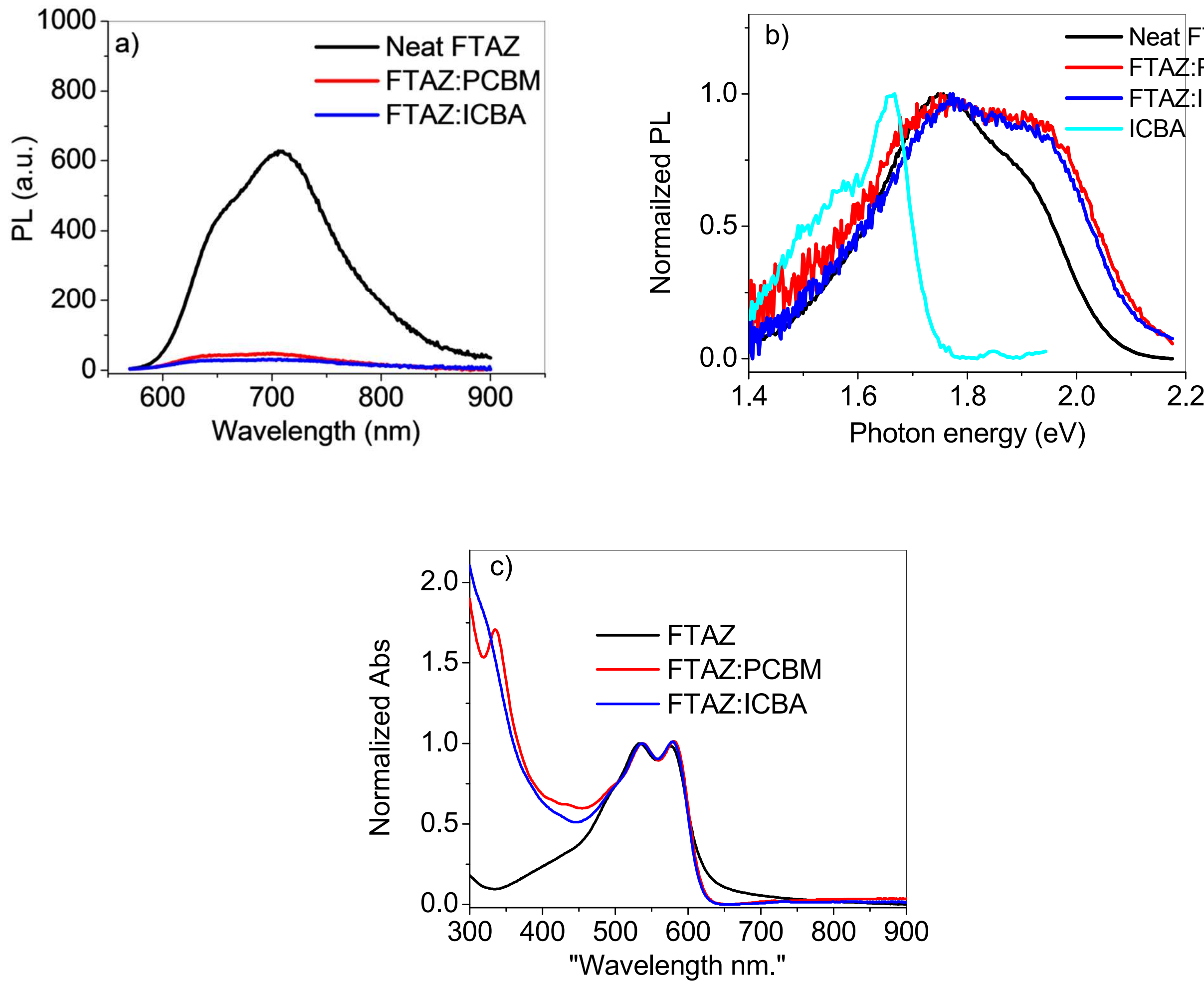

Figure S 8 a) Photoluminescence spectra of neat FTAZ and FT:PC and FT:IC films (thickness about 180 nm) b) Normalized PL of FTAZ, ICBA, FT:PC and FT:IC c) Normalized absorption spectra of FTAZ, FT:PC and FT:IC.

6. Scattering contrast function

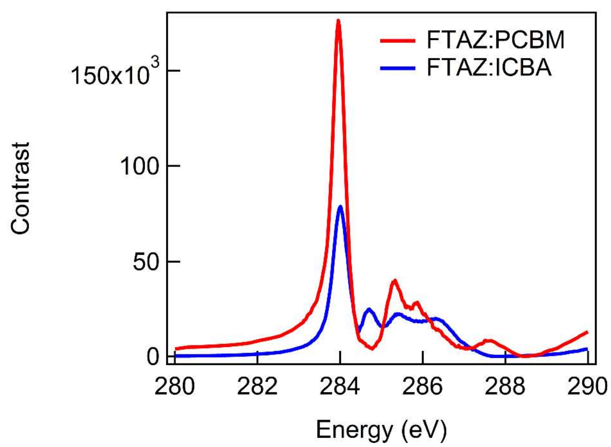

Figure S9. Compositional contrast between FTAZ and PCBM or ICBA as a function of incident X-ray energy. The compositional contrast is calculated by $C=E4(\Delta\delta2+\Delta\beta2)$, where E is the incident X-ray energy, $\Delta\delta$ is the difference of dispersive optical constants and $\Delta\beta$ is the difference of absorptive optical constants.

7. GIWAXS profiles of the pure materials

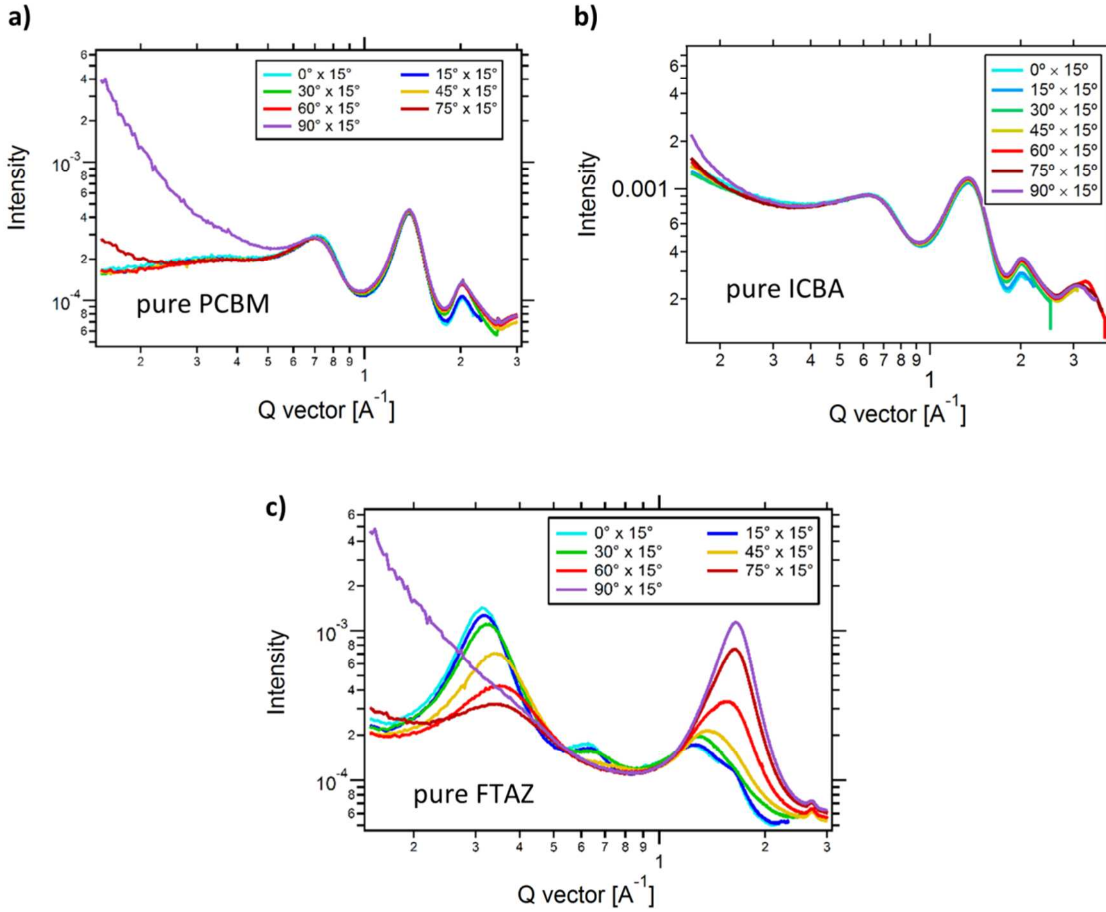

Figure S10 GIWAXS profiles of pure PCBM a), pure ICBA b) and pure FTAZ c) films along varying azimuthal angles from 0° (in-plane) to 90° (out-of-plane).

8. STXM images of isothermally annealed FT:PC and FT:IC at varying temperatures

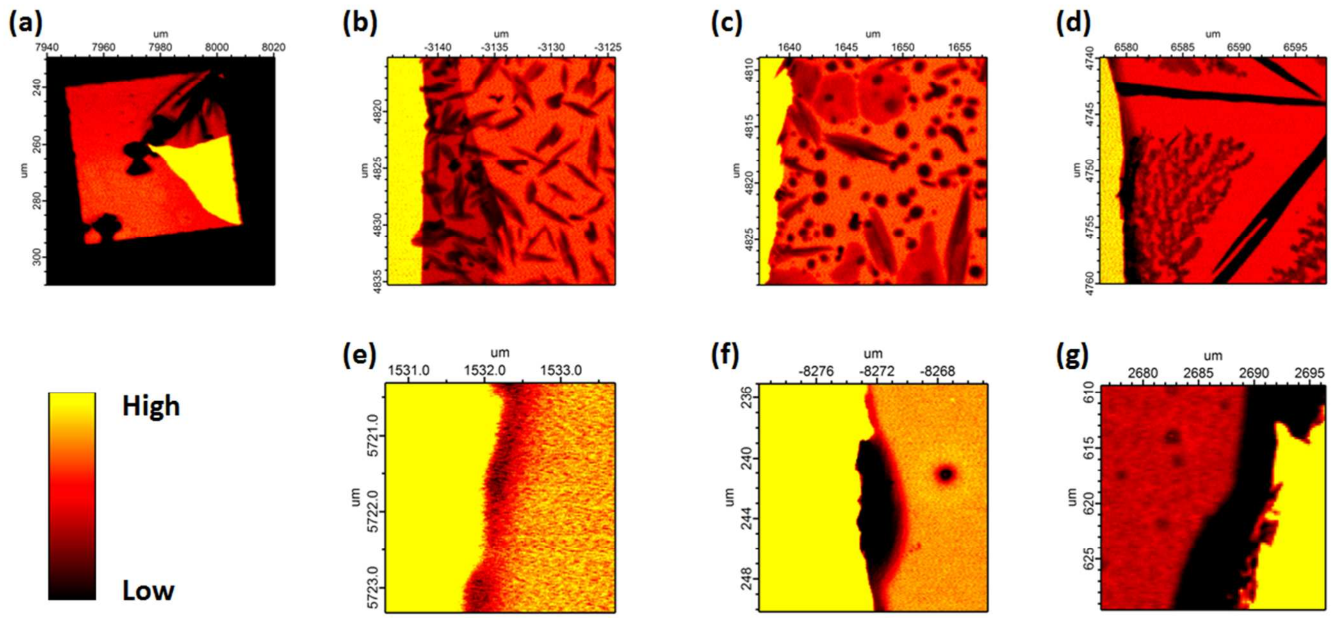

Figure S11. STXM images of isothermally annealed blends. The annealing temperatures were chosen at 100 °C, 140 °C and 170 °C for FT:PC (b - d) and FT:IC (e - g), respectively. (a) is the solvent annealed FT:PC blends, which shows consistent result with previous literature.[S1] Note that the field of view and intensity bar are intentionally set different across different images with the aim of providing clear identification of fullerene crystals.

[S1] Tumbleston, J. R.; Stuart, A. C.; Gann, E. ; You, W.; Ade, H. *Advanced Functional Materials* **2013**, *23*, 3463.

9. Thermal properties of PCBM, ICBA, FT:PC and FT:IC

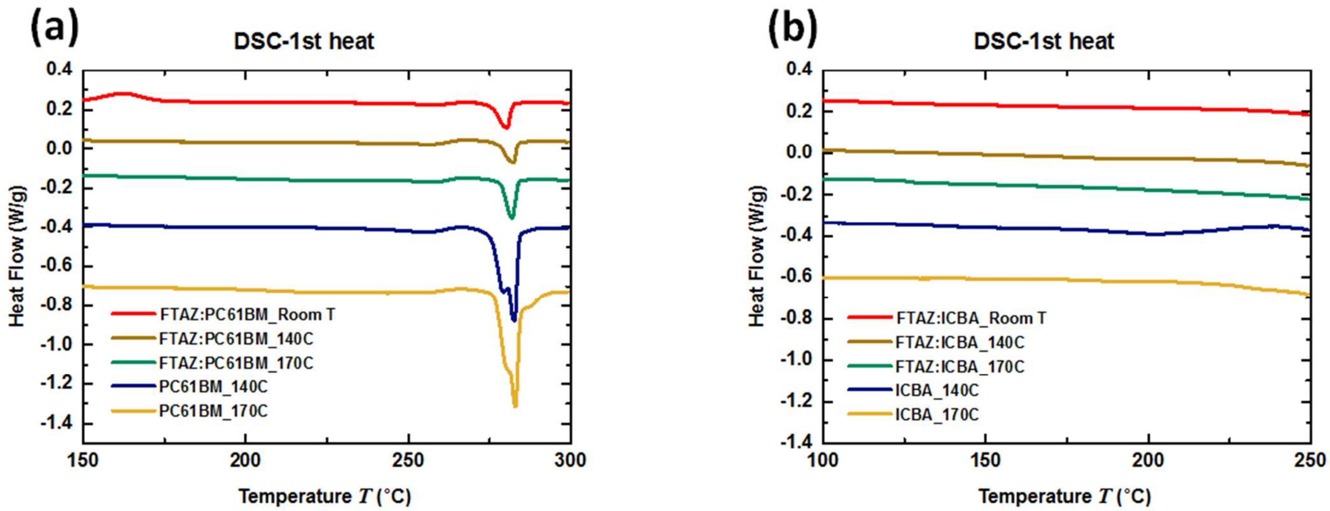

Figure S12. DSC scans of pure PCBM, pure ICBA, FT:PC and FT:IC isothermally annealed at varying temperatures for 3 days. Both pure and blend films were drop cast from CB solution.